Rh–Ni/CeO$_2$–Al$_2$O$_3$ catalysts for methane dry reforming

Marco Ocsachoque, Francisco Pompeo, Gloria Gonzalez *

Universidad Nacional de La Plata, Centro de Investigacion y Desarrollo en Procesos Cataliticos, 47 257, B1900AJK La Plata, Argentina

ARTICLE INFO

ABSTRACT

A series of Ni and Rh–Ni catalysts supported on Al$_2$O$_3$ modified by CeO$_2$ (3 and 5 wt%, Ce) was studied for CO$_2$ reforming of methane. Catalysts were characterized by hydrogen chemisorption, TPR, XRD, XPS, BET, TEM and dry reforming reaction tests. The influence of calcination temperature and Ce loading on activity and stability of mono and bimetallic samples was studied. The effect of Rh and Ce addition to Ni/a-Al$_2$O$_3$ catalyst improves the activity. Results show that the catalyst content 3%w/w Ce calcined at 650 °C, present higher reforming activity and stability than the unpromoted catalyst. The higher catalytic activity is attributed to the interaction between Rh and Ce phases, which has been verified by TPR experiments that improve the Rh dispersion and increase the catalyst active surface. The Rh addition on Ce–Al$_2$O$_3$ support increases the resistance to deactivation by carbon deposition.

1. Introduction

The methane dry reforming (DRM) has received considerable attention in recent years [1,2] mainly as an attractive route to produce synthesis gas. The low H$_2$/CO ratio obtained in this process is technologically interesting in the synthesis of liquid fuels by means of Fischer–Tropsch processes. This process is very important in the use of biomass as renewable energy source for biogas conversion (60% CH$_4$ and 40% CO$_2$) to synthesis gas. So, the biogas can be converted into a value-added commodity and can contribute to reduce CO$_2$ emissions to the atmosphere. An advantage of this process would be the possibility of use a big number of reserves of natural gas where together with CH$_4$, important amounts of CO$_2$ are found, and through the DRM the CO$_2$ will not be emitted into the atmosphere. The methane reforming can be an alternative source of hydrogen production for combustion cells.

Ni catalysts are the most used ones due to their low cost. However, the strong thermodynamic potential for carbon deposition and the high reaction temperatures limit their commercial application. The literature is consistent with the fact of attributing to noble metals [3–9] the high performance and low carbon deposition as catalysts for the dry reforming of methane, but their low availability and high cost restrict their use in large-scale processes. The modification of catalysts based on Ni by addition of low concentrations of noble metals leads to catalytic systems of accessible cost with good catalytic properties and low sensitivity to carbon forma-

tion. In previous works [10] we have noticed that the addition of low Rh contents on Ni/γ-Al$_2$O$_3$ catalysts improves the activity and stability of catalysts making them more convenient for their use at industrial scale. At the same time, the Ce has been reported as an effective promoter to prevent the metallic sintering, to favor the activity and the resistance to coke formation. A way to improve catalytic behavior of systems based on Ni has focused on the modification of support characteristics, and related with that, on the nature of metal-support interaction.

The aim of this work was to elucidate the role that fulfills the CeO$_2$ addition in Rh–Ni bimetallic catalysts supported on α-Al$_2$O$_3$ on the activity, stability and deactivation by carbon deposition during dry reforming of methane.

2. Experimental

The bimetallic catalysts containing 0.5% Rh and 5% Ni were prepared by impregnation at incipient wetness of the CeO$_2$-α-Al$_2$O$_3$ support with aqueous solutions of Cl$_3$Rh and Ni(NO$_3$)$_2$. First the support was impregnated with Rh and was calcined at 350 °C for 1 h. After, the Ni was additioned and calcined at 500 °C during 1 h. The modified support (CeO$_2$-α-Al$_2$O$_3$) was obtained by impregnation at pore volume of α-Al$_2$O$_3$ (S_{BET}: 5 m^2 g^{-1}), with CeO$_2$ (1, 3 and 5%w/w), previous drying at 100 °C and calcinations at 500 °C for 1 h. Ni monometallic catalysts were prepared with the same technique just for comparison. Samples were named Ni/Al, Ni/Ce(x)Al, Rh–Ni/Ce(x)Al, where x indicates the % w/w Ce content. Previous to the catalytic test, samples were in situ reduced in hydrogen stream at the reaction temperature for 1 h.

* Corresponding author. Tel.: +54 0221 4254277.
  E-mail address: mgg@quimica.unlp.edu.ar (G. Gonzalez).

Table 1
Catalysts characterization.

Catalyst	V_p (cm³/g)	Sg (m²/g)	A_{Ni} (m²/g$_{Ni}$)	D_{Ni}[a] (%)	D_{Rh}[a] (%)	dp$_{Ads}$ (nm)	dp$_{TEM}$ (nm)
Ni/Al (500)	0.017	5.8	7.12	1.72	–	59	34
Ni/Ce(3)Al(500)	0.026	6.0	26.7	3.50	–	31	38
Ni/Ce(5)Al(500)	0.031	7.64	22.8	3.36	–	32	–
Ni/Ce(5)Al (650)	0.046	13.03	27.4	4.00	–	25	–
RhNi/Ce(3)Al(500)	0.034	7.13	26.7	4.00	28	25	–
RhNi/Ce(5)Al(500)	0.033	8.53	27.8	4.70	32	23	29
RhNi/Ce(5)Al(650)	0.077	19.61	22.3	4.30	25	25	–

[a] H₂ chemisorption data.

Catalysts were characterized by X-ray diffraction (XRD), hydrogen chemisorption, temperature programmed reduction (TPR), TEM, X-ray photoelectron spectroscopy (XPS) and N₂ adsorption (BET), in order to correlate chemical and physical characteristics with catalytic properties focusing the attention on deactivation problems.

Structural characterization of catalysts was performed by XRD technique on a Philips PW 1740 equipment using CuKα radiation, under 30 mA current and 40 kV voltages and a continuous scan angle 2θ was selected from 5° to 70°.

Reducibility of the samples was determined by TPR technique on a conventional equipment. A 100 mg sample was loaded in a quartz reactor and heated from RT to 900 °C at 10 °C/min under 10% (v/v) H₂/N₂ stream at a flow rate of 20 cm³/min.

Metal dispersion was measured through H₂ pulse chemisorption in a flow conventional equipment. The monometallic Rh and Ni catalysts were reduced at 270 and 500 °C, respectively and then cooled down to R.T. under Ar. Then a H₂ in Ar mixture was pulsed for measuring the dispersion of Rh and Ni. A sequential H₂ pulse chemisorption methods were used to separately determine the dispersion of Rh and Ni in the bimetallic catalysts.

The BET surface area and pore volume distribution were measured by N₂ adsorption at −196 °C in an Accusorb 2100E Micromeritics analyzer. Samples were outgassed at 100 °C during 12 h before adsorption.

The surface chemical compositions of catalysts were determined using the XPS technique. Spectra were performed in a multi-technique system (SPECS) equipped with a dual Mg/Al X-ray source and a hemispherical PHOIBOS 150 analyzer operating in the fixed analyzer transmission (FAT) mode.

Catalytic runs was carried out in a fixed bed quartz reactor with on line chromatograph at temperatures between 650 and 750 °C and atmospheric pressure on a catalyst mass of 0.03 g. The reactor was fed with a gas flow rate of 100 cm³/min at two CH₄/CO₂ ratios of 0.5 and 1.2 using He as balance. The absence of diffusional controls was verified. Isothermal stability tests were performed during 20 h under reaction conditions (CH₄/CO₂ = 0.5, Temp = 650 °C) where, according thermodynamic data, the spontaneous carbon deposition would no occur. In the same temperature and time conditions but feeding the reactor with a CH₄/CO₂ = 1.2 molar ratio, it was possible to analyze the deactivation by carbon deposition. The amount and reactivity of carbon deposited on catalysts was determined by TGO and TPH techniques. The thermogravimetric analysis was carried out in a Shidmazu TG 50 thermobalance under air stream between 100 and 900 °C at a rate of 20 °C/min. TPH was performed on a conventional flow system under hydrogen stream between 100 and 900 °C at a heating rate of 5 °C/min. Experiments were performed over samples extracted from reactor after 20 h on stream.

3. Results and discussion

3.1. Characterization of catalysts

Table 1 shows the morphological properties of catalysts under study (BET area, pore volume, metal dispersions and Ni area). The addition of CeO₂ into the alumina produces important changes on textural parameters and Ni dispersion of the catalysts, which is evidenced in larger specific surface and important decrease of Ni particle size in the promoted monometallic as well as in the bimetallic catalyst. Catalysts promoted with Ce (3 or 5%w/w) have particle size smaller than the one corresponding to Ni/Al, which would indicate that the Ce addition increases the metallic dispersion in agreement with results of Wang and Lu [11]. The Ni particle size determined by TEM analysis using the average volume-area equation ($\sum n_i d_i^3 / \sum n_i d_i^2$) showed similar values for catalysts containing Ce.

The variation in the textural properties with the calcination temperature can be related to the stabilization effect of ceria on the surface area of alumina [12].

The XRD analysis of the different samples allowed identification of characteristic Ni peaks (JCPDS 87-0712) and CeO₂ fluorite structure (2θ = 28.5, 33.3, 47.5 and 56.4) and the remaining peaks correspond to α-Al₂O₃ (JCPDS 43-1484), as are shown in Fig. 1. The low Rh content impedes its identification by this technique.

Table 2 shows the values of Ni particle sizes in fresh and used samples reduced at 750 °C, determined by Scherrer equation. Mod-
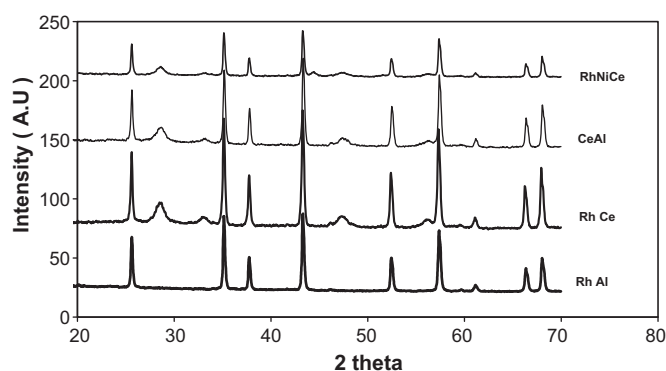

Fig. 1. XRD spectra of fresh catalysts.

Table 2
Ni Crystallite size of fresh and used catalysts.

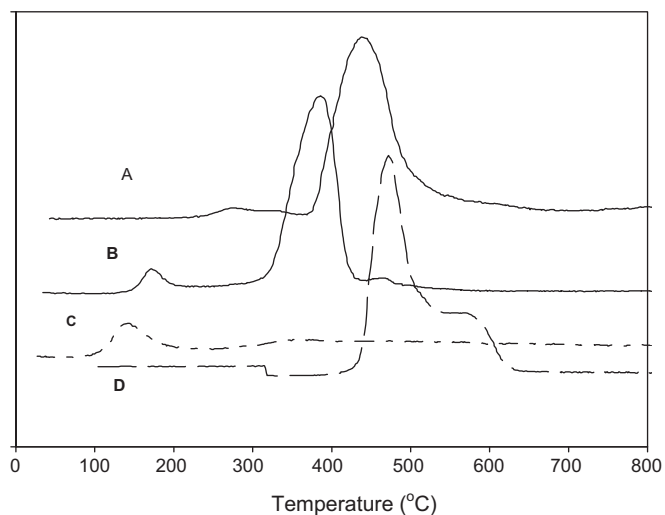| Catalysts	Crystallite size (nm)[a]	
	Fresh	Used
Ni/Al₂O₃	23	
Ni/Ce(3)Al	22	24
Ni-Rh/Ce(3)Al	20	23
Ni/Ce(5)Al	19	23
Ni-Rh/Ce(5)Al	20	24

[a] By Scherrer eq.

Fig. 2. TPR.

ifications were not practically observed in crystal sizes determined by XRD. They resulted very similar to the ones shown in Table 1, obtained by hydrogen chemisorption, for catalysts promoted by ceria.

Fig. 2 shows TPR profiles of mono and bimetallic catalysts. Results indicate that the Rh added to Ni/CeAl catalysts improves the Ni reducibility, decreasing the NiO reduction temperature from 442 to 388 °C. This effect can be attributed to H_2 spillover that is generated between the noble metal and the modified support with ceria [13,15]. The thermograms present a peak around 170 °C assigned to the reduction of isolated RhO_x species and the signal at

470 °C would correspond to the reduction of Rh that interacts with the support. The intermediate temperature range of the reduction of bimetallic catalysts can be attributed to a mixed coordination sphere of nickel and rhodium ions [16].

XPS analysis was used to determine the chemical composition of the catalysts surface and to better understand the nature of interaction between the dispersed metal species and the supporting oxides. The XPS spectra are shown in Fig. 3.

The Rh 3d spectrum of RhNi/CeAl (Fig. 3A) presents 2 peaks at 306.7 and 311.45 eV corresponding to Rh $3d_{5/2}$ and Rh $3d_{3/2}$ respectively. This doublet is assigned by Wang et al. [14] to the coexistence of species Rh^0 and $Rh^{+\simeq}$ indicating that it corresponds to an interaction between Rh and CeO_2. Garcia Fierro et al. [17] have proposed that the presence of $Rh^{\delta+}$ in a ceria doped catalyst can be associated with stabilization of ionic Rh species by the support which is related to the Ce^{3+}/Ce^{4+} redox properties of ceria. This effect facilitates electron transfer from Rh to CeO_2. The partially oxidized Rh promotes the CH_4 activation.

In the Ce 3d region, it is possible to notice that the Rh presence favors the Ce reduction. Signals between 881 and 884.9 eV correspond to Ce $3d_{3/2}$ and between 899 and 903 eV to Ce $3d_{5/2}$, respectively. Ce^{+3} and Ce^{+4} contributions are indicated in Fig. 3B and C for each sample. The lower intensity of Ce^{+4} peak with respect to the Ce^{+3} peak suggests that CeO_{2-x} ($0 > x > 0.5$) was formed by Rh and CeO_2 interaction during the reduction, coinciding with TPR data [18,19].

The spectra corresponding to Ni 2p region for Ni and NiRh catalysts after in situ H_2 treatment are illustrated in Fig. 3D and E. The Ni 2p region consisted of two maximums at 852.2 and 855.2 eV (with the satellite at 861.7) indicative of Ni^0 and Ni^{+2} species respectively. In the bimetallic catalyst (Fig. 3E) the fraction of Ni^0 is higher than in Ni/CeAl sample (Fig. 3E). From these data, it is possible to conclude that the Rh presence would favor the Ni reduction thus increasing the active phase [20–22].
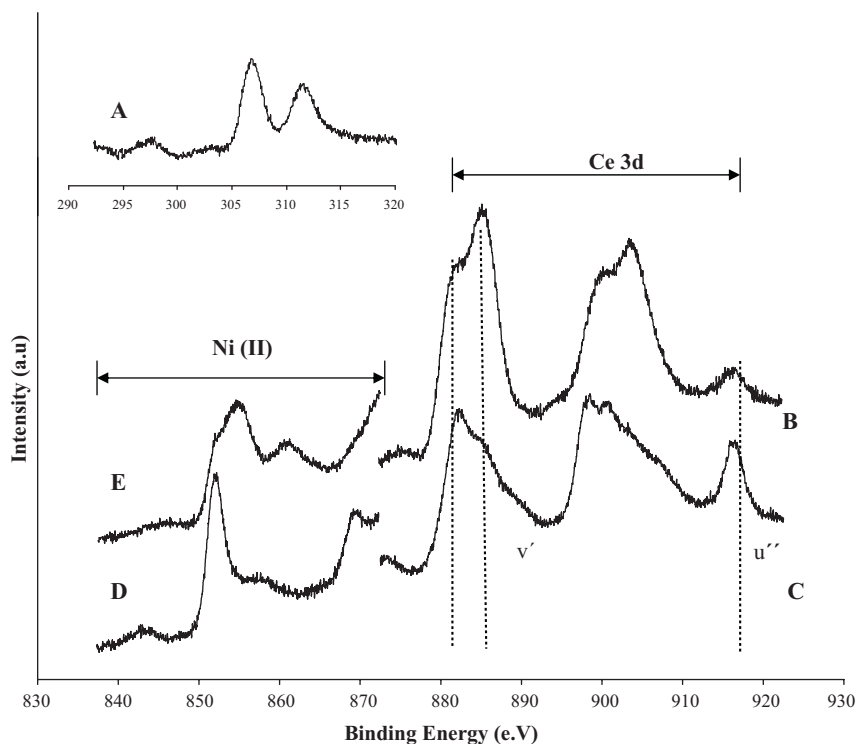

Fig. 3. XPS Spectra of catalysts reduced at 650 °C. (A) Rh 3d region of RhNi/CeAl. (B) Ce 3d region of RhNi/CeAl. (C) Ce 3d region of Ni/CeAl. (D) Ni 2p region of Ni/CeAl. (E) Ni 2p region of RhNi/CeAl.

Table 3
Catalytic activities after 1 h in reaction.

Catalyst	Temp			R_D
	650 °C	700 °C	750 °C	
	Methane conversion (%)			
Ni/Al	53	61	68	0.86
Ni/Ce(3%)Al	58	69	75	0.92
Rh–Ni(3%)/CeAl	71	80	85	0.98

3.2. Catalysts performance

Catalysts were evaluated in the reaction of dry reforming of methane in chemical control conditions analyzing the performance for 20 h. In order to compare the methane conversions, experiments were performed at the same space time and feed composition.

Table 3 shows the catalytic activity at 650, 700 and 750 °C for $CH_4/CO_2 = 0.5$ on Ni and Rh–Ni samples supported on CeO_2-α-Al_2O_3 and the unpromoted Ni/Al catalyst just for comparison. Ce and Rh additions have a positive impact on the activity, in agreement with a higher Ni dispersion in Ce promoted catalysts. Wang and Ruckenstein [7] reported that the activity depend significantly on Rh crystallite size on Rh/Al_2O_3 catalyst.

Stability tests and the effect of CeO_2 loading on catalysts are shown in Fig. 4. The methane conversion as function of time on stream is represented for a $CH_4/CO_2 = 0.5$ ratio in order to inhibit the carbon formation. The experiments were performed at 750 °C on Ni and Rh–Ni catalysts, promoted with 3 and 5%w/w Ce and calcined at 500 °C. The RhNi/Ce(3)Al catalyst showed higher activity and stability compared to other samples. The coexisting on the surface of Rh^o and $Rh^{\delta+}$ sites, as was observed by XPS, can be responsible of the higher performance of bimetallic catalyst. The monometallic Ni/Ce(5%)Al catalysts is the one that shows lower methane conversion, in agreement with the lower metallic surface area.

In order to analyze the effect of the Ce content, the Ce loading was increased from 1 to 5% for Ni and Rh–Ni samples, noticing that the activity order is the following; $Ce(3\%) \gg Ce(1\%) \approx Ce(5\%)$, in agreement with data reported recently for Ce promoted Pt/ZrO_2 catalysts [15]. These results suggest the higher promoting effect of 3% of Ce on the activity of catalysts studied.

The deactivation rate at 750 °C (R_D) defined as the ratio between methane conversion after 15 h and the conversion at 1 h in reaction is shown in Table 3. The support modification with Ce as well as the Rh addition as active phase increases the stability of the catalysts. At the end of 15 h in reaction the unpromoted Ni/Al catalyst lost 14% whereas the Ce promoted monometallic catalyst only lost 8% of its initial CH_4 activity. These results show the beneficial effect of Ce on the stability of promoted catalysts. For the bimetallic catalysts
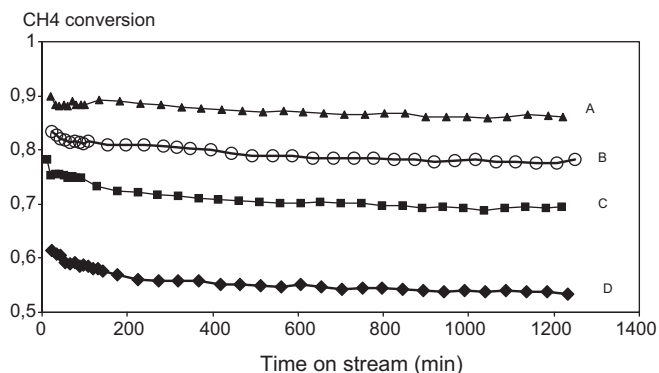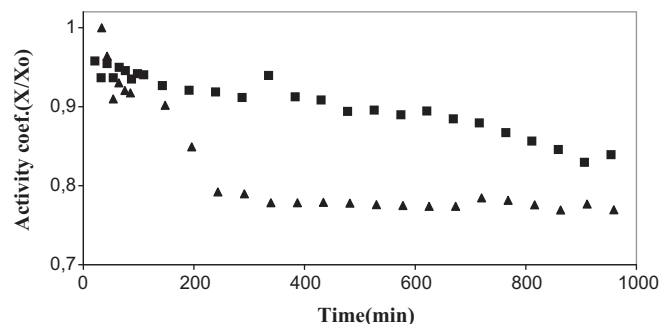

Fig. 5. Stability of RhNi/CeAl (■) and Ni/CeAl (▲) catalysts at 750 °C, CH_4/CO_2: 1.2.

the activity was quasy stable under all time on stream. Eriksson et al. [17] reported that certain interaction between Rh and Ce, as it was observed by our TPR and XPS data, produces the Rh dispersion increasing the catalyst active surface.

The effect of partial pressures of reagents and products was analyzed on the RhNi/Ce(3%)Al catalyst varying the partial pressures between 0.02 and 0.07 atm for the methane and 0.05 and 0.2 for CO_2. The partial pressure of H_2 was varied between 0.0 and 0.1. These experiments varying partial pressures showed that the methane conversion is constant with the increase of CH_4 partial pressure. Meanwhile the methane conversion decreases with the increase of the H_2 partial pressure and it is almost insensitive to variations of methane and CO_2 concentrations. According other studies [23–25] the first order in methane is also valid for our experimental data. CO_2 do not directly influence the reaction rate, although there may be indirect influence through the production of CO and H_2 via the shift reaction.

The H_2/CO ratio in the synthesis gas is lower than the stoichiometric value of the reaction, which suggests the contribution of the reverse water-gas shift reaction (RWGS). Wang et al. [14] proposes that Ce addition promotes the CO_2 dissociation in CO and superficial oxygen. Both facts lead to a lower H_2/CO molar ratio.

The temperature effect in the 650–750 °C range on the activity of catalysts was determined by means of Arrhenius equation indicating an apparent activation energy equal to 37 kJ/mol for the RhNi/CeAl catalyst and a value of 42 kJ/mol for Ni/CeAl. Since the difference of apparent activation energy values is not so marked for both samples, it is possible to infer that the reaction mechanism is the same one.

3.3. Effect of CH_4/CO_2 ratio

In order to analyze the reaction with the most representative feed conditions for the industrial process, catalytic tests were carried out on samples containing 3%w/w Ce, for a $CH_4/CO_2 = 1.2$ molar ratio at 650 °C. When the CH_4/CO_2 ratios are higher than 1, the methane is found in excess and the carbon formed by the methane decomposition ($CH_4 \rightarrow C + H_2$) can be deposited on the catalytic surface deactivating the active phase. Under these feed conditions, bimetallic sample (RhNi/CeAl) presents an activity decrease (10.6%) during the 15 h catalytic test and the monometallic catalyst (Ni/CeAl) shows a highest deactivation (26%) in the first 4 h in reaction. Increasing the reaction temperature at 750 °C, at the same molar feed ratio, the behavior is similar although the deactivation degree is lower. These results suggest that while carbon formation is always favored thermodynamically there is a competing kinetic effect, since the reaction is endothermic, at lower temperature there is not sufficient energy to both initiate reforming and carbon gasification, however at high temperature there is sufficient energy and gasification carbon reaction can be responsible of lower deactivation degree at higher temperature [26].

Fig. 4. Catalytic stability at 750 °C, $CH_4/CO_2 = 0.5$. (A) RhNi/Ce(3%)Al, (B) RhNi/Ce(5%)Al, (C) Ni/Ce(3%)Al, and (D) Ni/Ce(5%)Al.
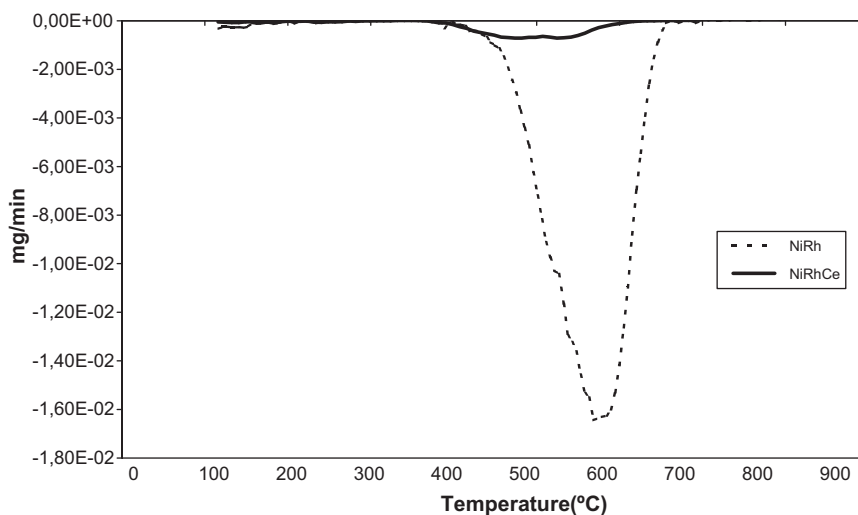
Fig. 6. TGO analysis of bimetallic catalysts.

The activity coefficient defined as a ratio between the activity at time t with respect to the initial activity is plotted in Fig. 5 as function of time on stream for RhNi/Ce(3)Al catalyst. During the 15 h test the Ni monometallic catalyst showed a higher deactivation compared with the RhNi catalyst although this last one does not avoid activity fall through time. As the crystal size is not practically modified after 15 h in reaction (Table 2), it is not possible to suppose that the Ni sintering is the potential deactivation cause. Considering that under these reaction conditions the carbon formation is thermodynamically favorable, samples extracted from the reactor after 15 h were treated in a thermobalance in air stream (TGO) to determine the quality and amount of deposited carbon.

3.4. Characterization of deposited carbon

The carbon content deposited on samples extracted from the reactor after 15 h was determined by thermogravimetry analysis on air stream at programmed temperature. Analyzing the DTG curves, shown in Fig. 6, it can be observed that the oxidation of carbonaceous species starts at 300 °C showing maximums at 500 and 600 °C. The signal around 500 °C would be related with whisker like filamentous carbon. Considering that the formation of whiskers is responsible for the destruction of the catalyst structure, it is important to inhibit their formation especially in industrial operations. Table 4 gives the content (%w/w) of carbon deposited on the bimetallic catalysts with and without Ce. It is evident that in the doped Ce catalyst decreases the carbon deposition but did not eliminate it. Catalysts promoted with 3% w/w CeO_2 present lower carbon deposition than the ones that contain 5% CeO_2. In Fig. 7 the TEM image of the used RhNi/CeAl catalyst provide clear evidence that the carbon formed during the reaction was in the form of filamentous whiskers. Although the possibility of smaller amount of carbon blocking active sites could not be excluded. It is widely known that filamentous carbon is formed on supported Ni catalysts by superficial intermediates ($CH_2 \Leftrightarrow C_{ads} + 2H_2$) that act as precur-

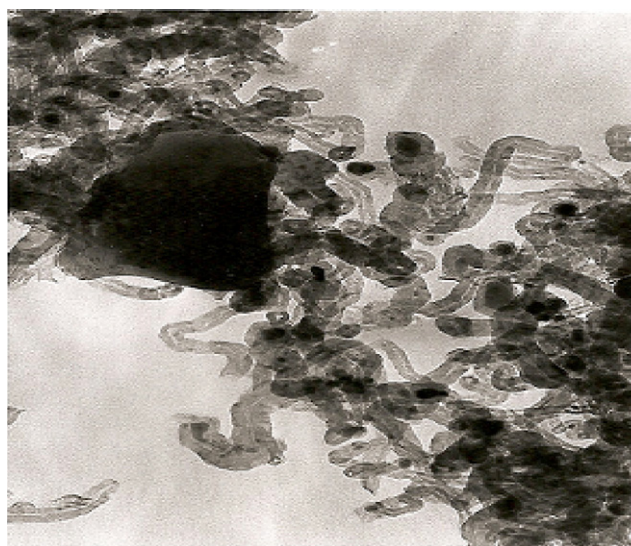**Fig. 7.** TEM image of the used RhNi/CeAl catalyst.

sors for different carbon types ($C_{ads} \rightarrow$ non-stoichiometric carbon, encapsulating carbon whisker) and a minimum assembly of metallic atoms is requires for the formation of surface species [27–30]. Probably, the CeO_2 favors the metallic dispersion and inhibits the formation of these assemblies improving the resistance to carbon formation. On the other hand, the couple Ce^{+4}/Ce^{+3} and $Rh^o/Rh^{\rightleftharpoons+}$ determined by XPS facilitate the activation of CH_4 and CO_2 and promotes carbon elimination.

4. Conclusions

The effect of α-Al_2O_3 modified by CeO_2 on the Rh–Ni/CeAl catalysts was investigated. It was found that these catalysts present good stability and activity for the dry reforming of methane at 650–750 °C. The higher activity and the resistance to carbon formation in the RhNi/Ce(3)Al_2O_3 catalyst would be associated with the presence of the redox couple Ce^{+4}/Ce^{+3} and $Rh^o/Rh^{\rightleftharpoons+}$ and to higher dispersion of the active phase on the CeAl.

Table 4
Carbon deposition at 650 °C.

Catalyst	$C_{dep.}$% (w/w)
RhNi/Al	19.10
RhNi/Ce(3)Al	2.45
RhNi/Ce(5)Al	4.40

Acknowledgements

References

[1] M.C.J. Bradford, M.A. Vannice, Catal. Rev. Sci. Eng. 41 (1999) 1.
[2] J.R.H. Ross, A.N.J. van Keulen, M.E.S. Hegarty, K. Seshan, Catal. Today 30 (1996) 193.
[3] M.M.V.M. Souza, D.A.G. Aranda, M. Schmal, J. Catal. 204 (2001) 498.
[4] M.C.J. Bradford, M.A. Vannice, J. Catal. 173 (1998) 157.
[5] S.M. Williams, F.B. Noronha, G. Fendley, D.E. Resasco, J. Catal. 194 (2000) 240.
[6] P.P. Silva, F.A. Silva, H. Souza, A.G. Lobo, L.V. Mattos, F.B. Noronha, C.E. Hori, Catal. Today 101 (2005) 31.
[7] H.Y. Wang, E. Ruckenstein, Appl. Catal. A 204 (2000) 143.
[8] A. Erdőhelyi, K. Fodor, T. Szailer, Appl. Catal. B 53 (2004) 153.
[9] P.G. Shulz, M.G. González, C.E. Quincoces, C. Gigola, Ind. Eng. Chem. Res. 44 (2005) 9020.
[10] M.A. Ocsachoque, C.E. Quincoces, M.G. González, Stud. Surf. Sci. Catal. 167 (2007) 397.
[11] S. Wang, G.Q. Lu, Appl. Catal. B 19 (1998) 267.
[12] R. Blom, I.M. Dahl, A. Slagtern, B. Sortland, A. Spjelkavik, E. Tangstad, Catal. Today 21 (1994) 535.
[13] A. Trovarelli, C. De Leitenburg, g. Dolcetti, J.L. Lorca, J. Catal. 151 (1995) 111.
[14] R. Wang, H. Xu, X. Liu, Q. Ge, W. Li, Appl. Catal. A 305 (2006) 204.
[15] S. Ozkara-Aydinoglu, E. Ozenkoy, A. Erhan Aksoylu, Int. J. Hydrogen Energy 34 (2009) 9711.
[16] W.K. Józwiak, M. Nowosielska, J. Rynkowski, Appl. Catal. A 280 (2005) 233.
[17] S. Eriksson, S. Rojas, M. Boutonnet, J.L.G. Fierro, Appl. Catal. A 326 (2007) 8.
[18] J.J. Strohm, J. Zheng, C. Song, J. Catal. 238 (2006) 309.
[19] J. Fang, X.Z. Bi, D.J. Si, Z.Q. Jiang, W.X. Huang, Appl. Surf. Sci. 253 (2007) 8952.
[20] J. Wang, M. Shen, J. Wang, M. Wang, W. Wang, J. Ma, L. Jia, Catal. Lett. 140 (2010) 38.
[21] W.J. Shan, M. Fleys, F. Lapicque, D. Swierczynskiu, A. Kiennemam, Y. Simon, P.M. Marquuaire, Appl. Catal. A 311 (2006) 24.
[22] G. Poncelet, M.A. Centeno, R. Molina, Appl. Catal. A 288 (2005) 232.
[23] C.E. Quincoces, M.G. González, Chinese J. Chem. Eng. 9 (2) (2001) 190.
[24] J.M. Wei, E. Iglesas, J. Catal. 225 (2004) 116.
[25] M. Maestri, D.G. Vlachos, A. Berretta, G. Groppi, E. Tronconi, J. Catal. 259 (2008) 211.
[26] F. Barrai, T. Jackson, N. Whitmore, M.J. Castaldi, Catal. Today 129 (2007) 391.
[27] J.R. Rostrup-Nielsen, J. Catal. 85 (1984) 31.
[28] M. Demicheli, E. Ponzi, O. Ferretti, A. Yeramián, Chem. Eng. J. 46 (1991) 129.
[29] D. Duprez, M. Demicheli, P. Marecot, J. Barbier, O. Ferretti, E. Ponzi, J. Catal. 124 (1990) 324.
[30] M.G. González, E.N. Ponzi, O.A. Ferretti, C.E. Quincoces, P. Marecot, J. Barbier, Adv. Sci. Technol. 18 (2000) 541.